

## Supporting Information

# Magnetic and Photo-physical Investigations in Dysprosium and Ytterbium Complexes Involving the 4,5-ethylendioxy-4',5'-bis(2-pyridyl-N-oxidemethylthio)tetrathiafulvalene Ligand

Khaled Soussi,<sup>a</sup> Julie Jung,<sup>a</sup> Fabrice Pointillart,<sup>\*a</sup> Boris Le Guennic,<sup>a</sup> Bertrand Lefevre,<sup>a</sup> Stéphane Golhen,<sup>a</sup> Olivier Cador,<sup>a</sup> Yannick Guyot,<sup>b</sup> Olivier Maury,<sup>c</sup> Lahcène Ouahab<sup>a</sup>

<sup>a</sup> Institut des Sciences Chimiques de Rennes UMR 6226 CNRS-UR1, Université de Rennes 1, 35042 Rennes Cedex, France.

<sup>b</sup> Université Claude Bernard Lyon 1, Institut Lumière Matière, UMR 5306 CNRS-Université Lyon 1, 10 rue Ada Byron, 69622 Villeurbanne Cedex, France

<sup>c</sup> Laboratoire de Chimie de l'ENS-LYON-UMR 5182, 46 Allée d'Italie, 69364 Lyon Cedex 07.

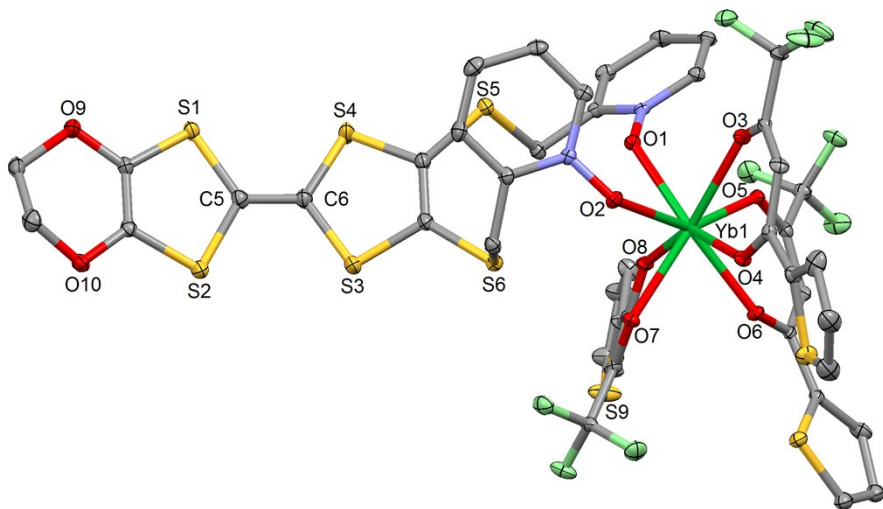


**Figure S1.** ORTEP view of the mononuclear complex  $[\text{Yb}(\text{tta})_3(\text{L})]$  (**3**). Thermal ellipsoids are drawn at 30% probability. Hydrogen atoms and dichloromethane molecules are omitted for clarity.

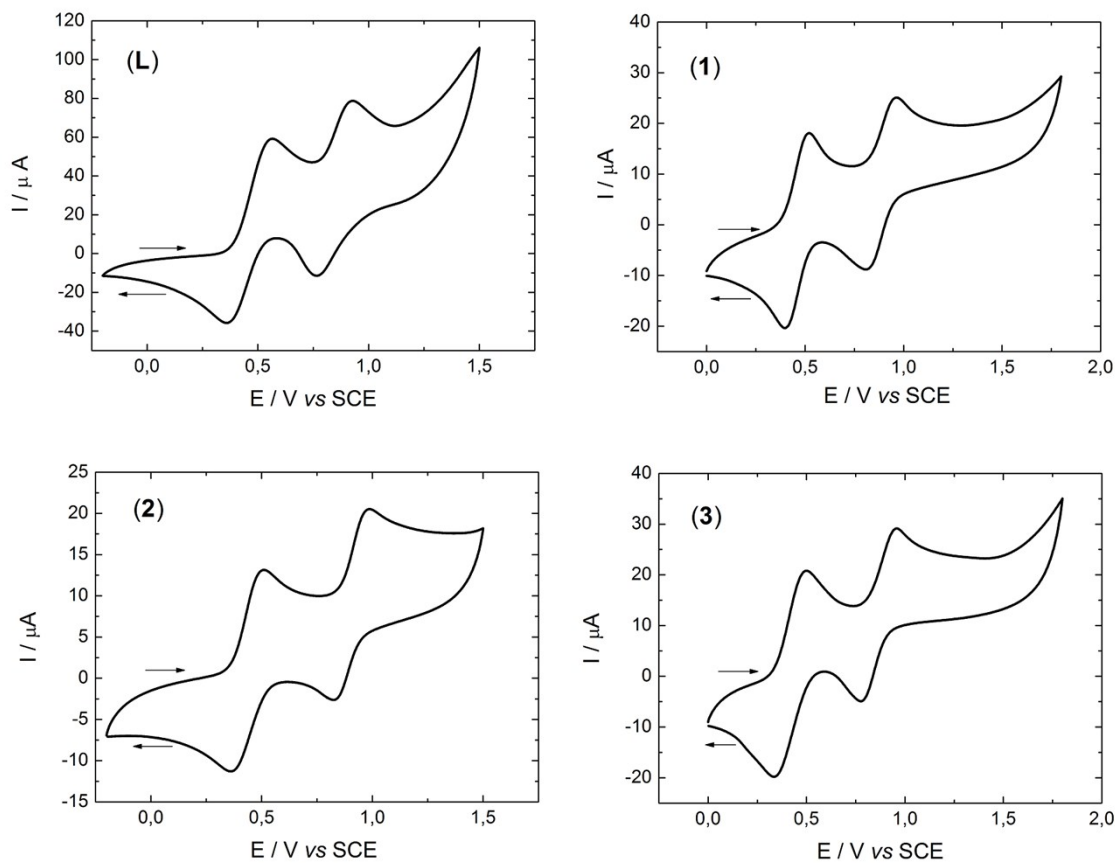


**Figure S2.** Cyclic voltammetry of the ligands **L** and representative complexes **1-3** in  $\text{CH}_2\text{Cl}_2$  at a scan rate of  $100 \text{ mV.s}^{-1}$ . The potentials were measured versus a saturated calomel electrode (SCE); Pt wire as the counter electrodes.

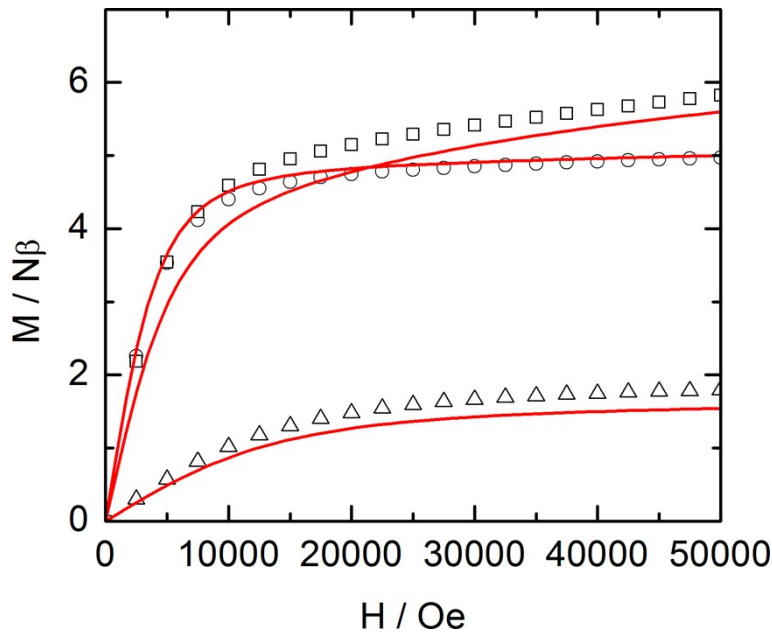


**Figure S3.** Magnetization curves measured at 2 K for **1** (circles), **2** (squares) and **3** (triangles). Simulated curves from *ab-initio* calculations are represented in full red lines.

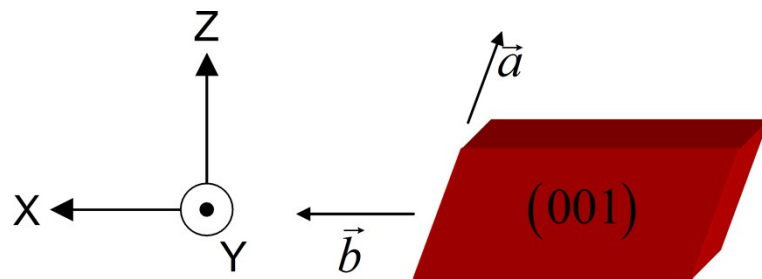


**Figure S4.** Oriented single crystal of **1** with the XYZ crystal reference frame.

The angular dependence of the magnetization was measured in the three orthogonal planes of an oriented single-crystal. Then, the molar magnetic susceptibility was fitted with:

$$\chi_M T = \frac{MT}{H} = \chi_{M_{\alpha\alpha}} T \cos^2 \theta + 2\chi_{M_{\alpha\beta}} T \sin \theta \cos \theta + \chi_{M_{\beta\beta}} T \sin^2 \theta \quad \text{Eq. S1}$$

where  $\alpha$  and  $\beta$  are the directions X, Y and Z in a cyclic permutation and  $\theta$  is the angle between  $H$  and  $\alpha$  direction.

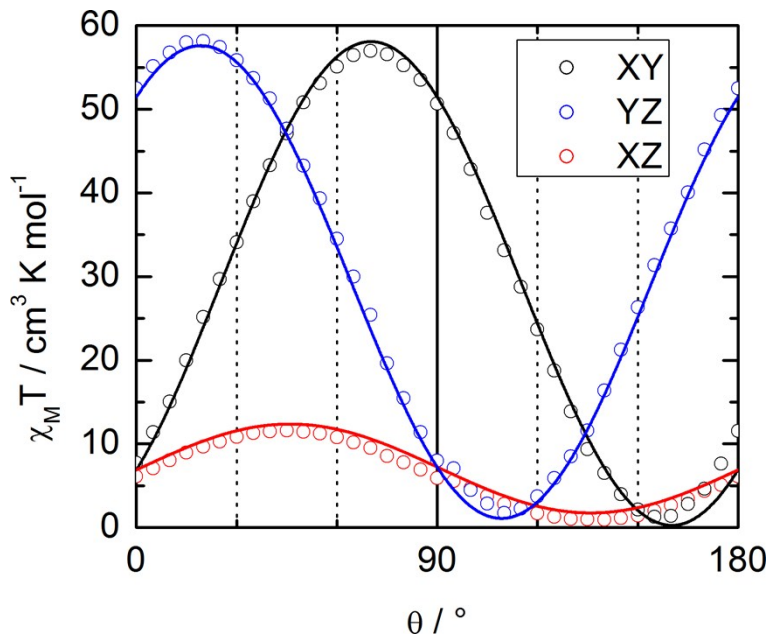


**Figure S5.** Angular dependence of  $\chi_M T$  of a single crystal of **1** rotating in three perpendicular planes with  $H=1$  kOe at 2 K. Best fitted curves in full lines with Eq. 1.

The molar magnetic susceptibility tensor of **1** in the crystal frame (XYZ) is:

$$\chi_M T = \begin{pmatrix} 6.893 & 18.418 & 5.307 \\ 18.418 & 51.459 & 17.588 \\ 5.307 & 17.588 & 7.242 \end{pmatrix} \text{cm}^3 \text{K mol}^{-1}$$

The principal values and directions of the susceptibility tensor for **1** in the XYZ crystal frame are obtained by diagonalization:

$$\chi_{xx} T \begin{pmatrix} 0.763 \\ -0.434 \\ 0.478 \end{pmatrix} = -0.264, \quad \chi_{yy} T \begin{pmatrix} 0.318 \\ 0.897 \\ 0.306 \end{pmatrix} = 64.015, \quad \chi_{zz} T \begin{pmatrix} -0.562 \\ -0.083 \\ 0.823 \end{pmatrix} = 1.843 \text{ cm}^3 \text{K mol}^{-1}$$

The negative value is physically meaningless. It is due to the experimental error in the alignment of the single crystal. The error with respect to the most magnetic direction is less than 1%. Taking into account the fact that there are two Dy(III) in a molecule the following principal  $g$  values are obtained for **1** in the  $1/2$  effective spin model :  $g_x=1.187$ ,  $g_y=18.47$  and  $g_z=3.134$ .

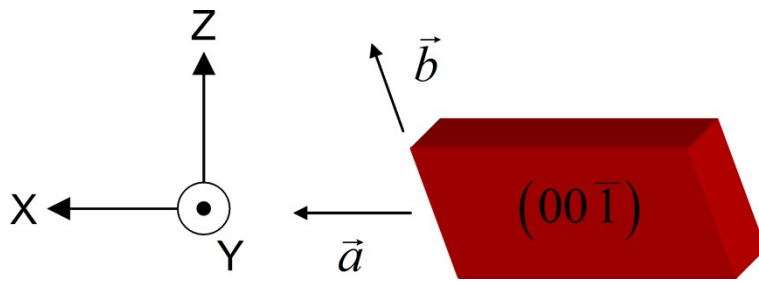


**Figure S6.** Oriented single crystal of **2** and **3** with the XYZ crystal reference frame.

The angular dependence of the magnetization was measured in the three orthogonal planes of oriented single-crystals. Then, the molar magnetic susceptibilities have been fitted with Eq. S1

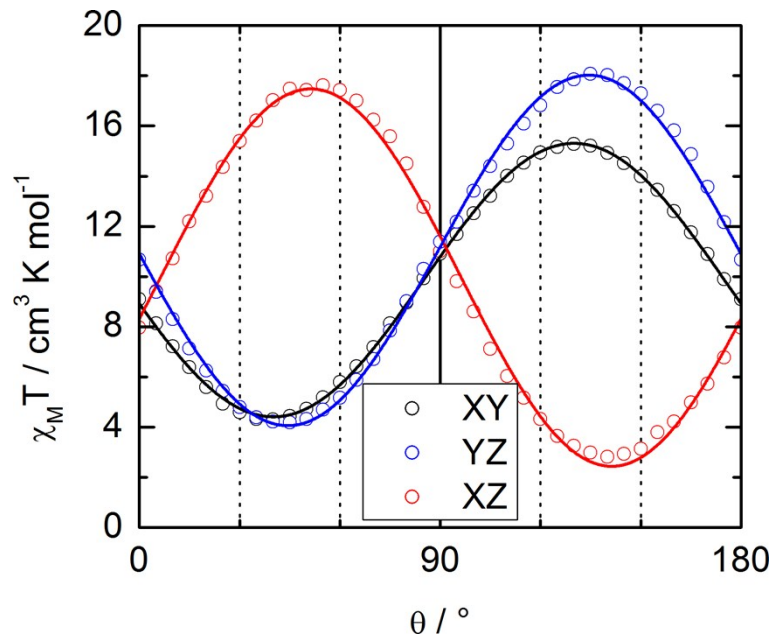


**Figure S7.** Angular dependence of  $\chi_M T$  of a single crystal of **2** rotating in three perpendicular planes with H=1 kOe at 2 K. Best fitted curves in full lines with Eq. 1.

The molar magnetic susceptibility tensor of **2** in the crystal frame (XYZ) is:

$$\chi_M T = \begin{pmatrix} 8.778 & -5.338 & 7.424 \\ -5.338 & 10.945 & -6.980 \\ 7.424 & -6.980 & 11.142 \end{pmatrix} \text{cm}^3 \text{K mol}^{-1}$$

The principal values and directions of the susceptibility tensor for **2** in the XYZ crystal frame are obtained by diagonalization:

$$\chi_{xx} T \begin{pmatrix} -0.485 \\ -0.811 \\ -0.330 \end{pmatrix} = 4.909, \quad \chi_{yy} T \begin{pmatrix} -0.701 \\ 0.134 \\ 0.701 \end{pmatrix} = 2.379, \quad \chi_{zz} T \begin{pmatrix} 0.523 \\ -0.571 \\ 0.633 \end{pmatrix} = 23.578 \text{ cm}^3 \text{K mol}^{-1}$$

Principal  $g$  values are obtained for **2** in the  $\frac{1}{2}$  effective spin model:  $g_x=7.24$ ,  $g_y=5.04$  and  $g_z=15.86$ .

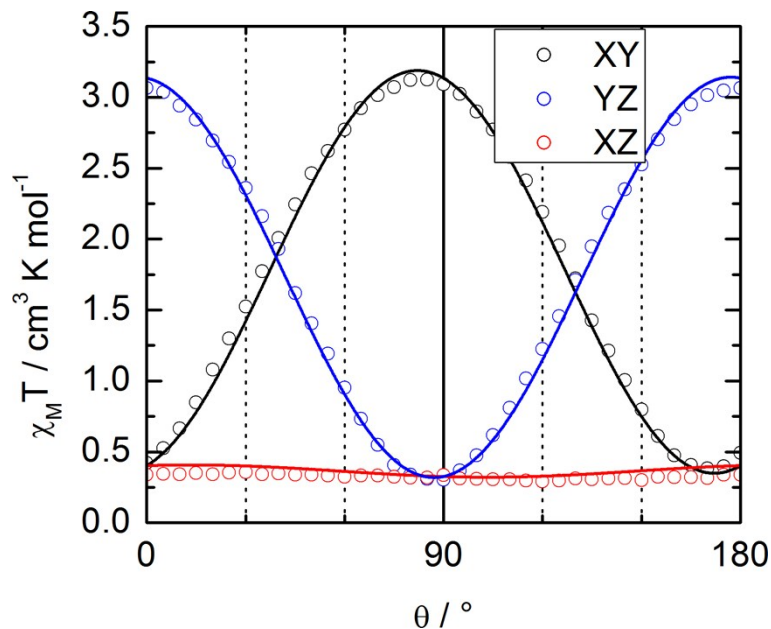


**Figure S8.** Angular dependence of  $\chi_M T$  of a single crystal of **3** rotating in three perpendicular planes with  $H=10$  kOe at 2 K. Best fitted curves in full lines with Eq. 1.

The molar magnetic susceptibility tensor of **3** in the crystal frame (XYZ) is:

$$\chi_M T = \begin{pmatrix} 0.403 & 0.388 & 0.019 \\ 0.388 & 3.135 & -0.141 \\ 0.019 & -0.141 & 0.326 \end{pmatrix} \text{cm}^3 \text{K mol}^{-1}$$

The principal values and directions of the susceptibility tensor for **2** in the XYZ crystal frame are obtained by diagonalization:

$$\chi_{xx} T \begin{pmatrix} -0.137 \\ -0.989 \\ 0.048 \end{pmatrix} = 3.196, \quad \chi_{yy} T \begin{pmatrix} 0.820 \\ -0.086 \\ 0.566 \end{pmatrix} = 0.376, \quad \chi_{zz} T \begin{pmatrix} 0.556 \\ -0.117 \\ -0.823 \end{pmatrix} = 0.293 \text{ cm}^3 \text{K mol}^{-1}$$

Principal  $g$  values are obtained for **2** in the  $\frac{1}{2}$  effective spin model:  $g_x=5.84$ ,  $g_y=2.00$  and  $g_z=1.77$ .

### Extended Debye model.

$$\chi_M' = \chi_S + (\chi_T - \chi_S) \frac{1 + (\omega\tau)^{1-\alpha} \sin\left(\alpha \frac{\pi}{2}\right)}{1 + 2(\omega\tau)^{1-\alpha} \sin\left(\alpha \frac{\pi}{2}\right) + (\omega\tau)^{2-2\alpha}}$$

$$\chi_M'' = (\chi_T - \chi_S) \frac{(\omega\tau)^{1-\alpha} \cos\left(\alpha \frac{\pi}{2}\right)}{1 + 2(\omega\tau)^{1-\alpha} \sin\left(\alpha \frac{\pi}{2}\right) + (\omega\tau)^{2-2\alpha}}$$

With  $\chi_T$  the isothermal susceptibility,  $\chi_S$  the adiabatic susceptibility,  $\tau$  the relaxation time and  $\alpha$  an empiric parameter which describe the distribution of the relaxation time. For SMM with only one relaxing object  $\alpha$  is close to zero. The extended Debye model was applied to fit simultaneously the experimental variations of  $\chi_M'$  and  $\chi_M''$  with the frequency  $f$  of the oscillating field ( $\omega = 2\pi\nu$ ). The best fitted parameters  $\tau$ ,  $\alpha$ ,  $\chi_T$ ,  $\chi_S$  are listed in Table S1 and S2 with the coefficient of determination  $R^2$ .

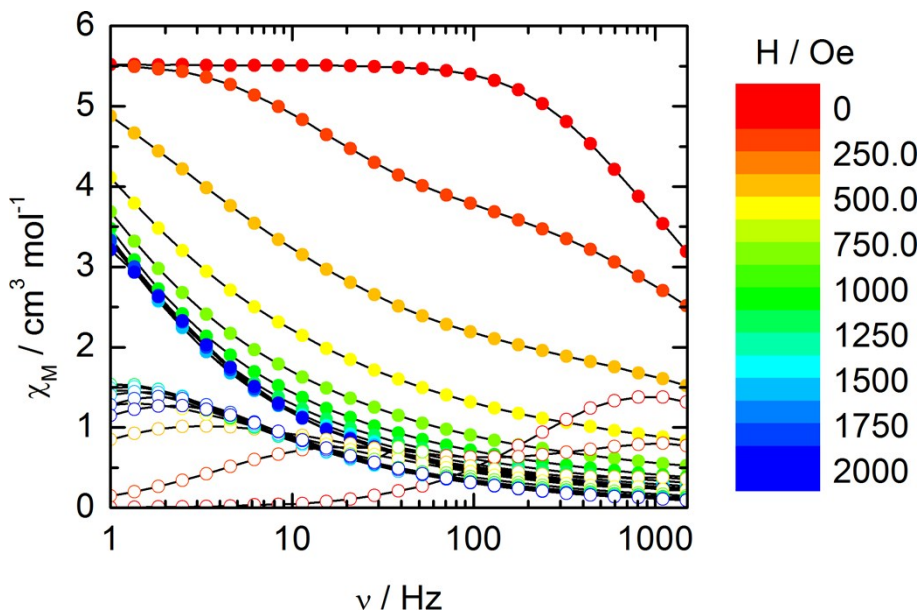


**Figure S9.** Magnetic field and frequency dependences of the two components of the ac susceptibility ( $\chi_M'$  in full symbols and  $\chi_M''$  in empty symbols) for **1** measured at 2 K.

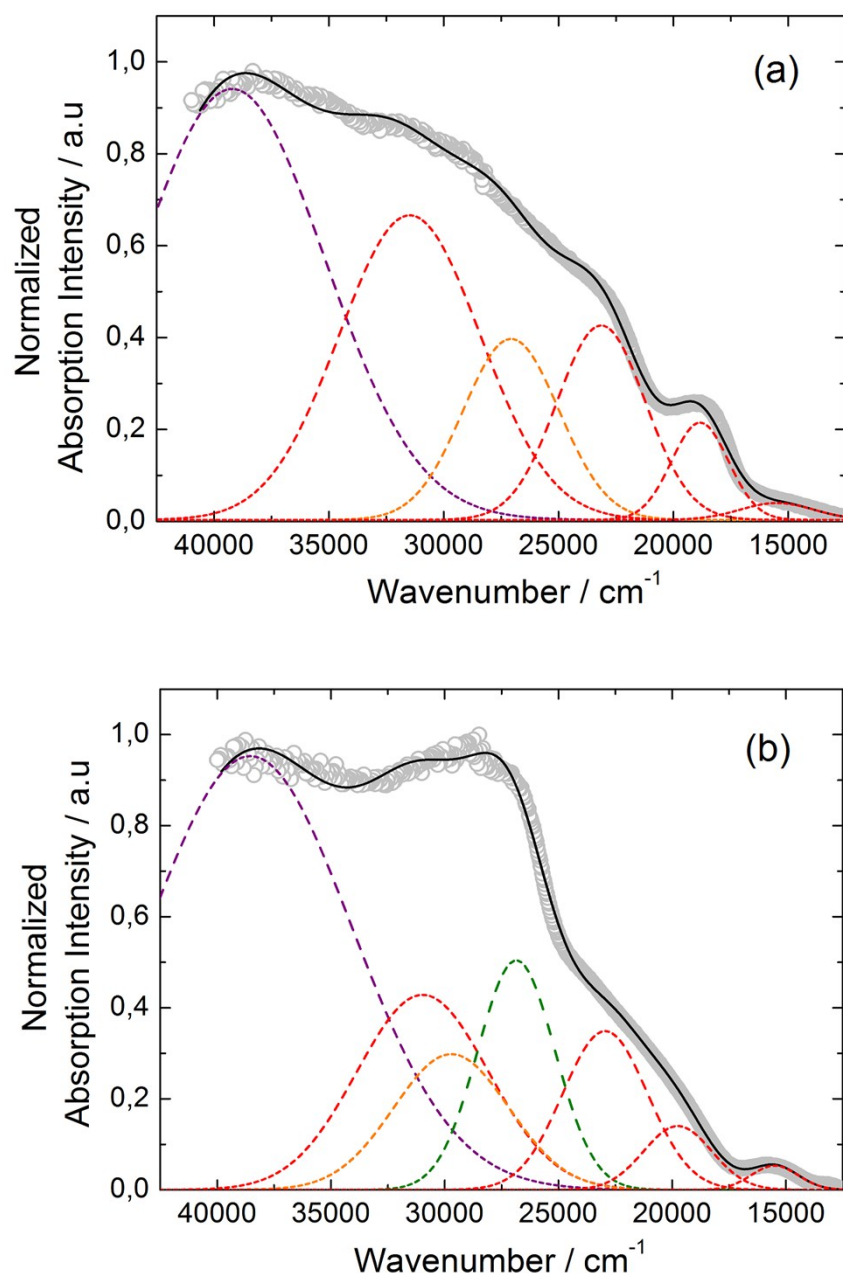


**Figure S10.** Experimental UV-visible absorption spectra in solid-state (KBr pellets) of compounds **L** (a) and **3** (b) (open gray circles). Respective Gaussian decompositions (dashed lines) and best fit (full black line), R = 0.9993 for **L** and R = 0.9992 for **3**. The red, orange, green and purple dashed lines represent the intra-ligand charge transfer, intra-TTF, intra-tta and intra-ligand absorption bands, respectively.

**Table S1.** Computed energy splitting ( $\text{cm}^{-1}$ ) of the  ${}^6\text{H}_{15/2}$  multiplet and weights of the  $\pm M_J$  components of the ground-state wavefunction for the Dy complexes **1** and **2**.

	Energy splitting of the ${}^6\text{H}_{15/2}$ multiplet								$\pm MJ$ weights of the GS wavefunction
<b>1</b>	0	80	98	113	152	194	206	502	0.96  $\pm 15/2$ >; 0.02  $\pm 9/2$ >; 0.01  $\pm 11/2$ >
<b>2</b>	0	15	62	93	114	154	217	367	0.69  $\pm 15/2$ >; 0.06  $\pm 11/2$ >; 0.04  $\pm 5/2$ >; 0.04  $\pm 1/2$ >

**Table S2.** Best fitted parameters ( $\chi_T$ ,  $\chi_S$ ,  $\tau$  and  $\alpha$ ) with the extended Debye model for **1** at 0 Oe in the temperature range 1.8-6 K.

T / K	$\chi_T / \text{cm}^3 \text{ mol}^{-1}$	$\chi_S / \text{cm}^3 \text{ mol}^{-1}$	$\alpha$	$\tau / \text{s}$	$R^2$
1.8	6.16692	2.46636	0.10721	2.07E-04	0.99985
2	5.5357	2.08717	0.13166	1.87E-04	0.99992
2.2	5.02009	1.92262	0.13218	1.87E-04	0.99991
2.4	4.62149	1.76042	0.13422	1.80E-04	0.9999
2.6	4.26258	1.63528	0.13076	1.74E-04	0.99991
2.8	4.08904	1.58583	0.12261	1.72E-04	0.99992
3	3.81569	1.49885	0.11906	1.66E-04	0.99993
3.5	3.26307	1.32174	0.10624	1.51E-04	0.99993
4	2.84822	1.21266	0.0836	1.36E-04	0.99993
4.5	2.53199	1.12174	0.06991	1.20E-04	0.99998
5	2.2827	1.03378	0.04976	1.02E-04	0.99999
5.5	2.07337	0.98218	0.02817	8.46E-05	0.99999
6	1.9015	1.05274	0.00101	7.69E-05	0.99999

**Table S3.** Best fitted parameters ( $\chi_T$ ,  $\chi_S$ ,  $\tau$  and  $\alpha$ ) with the extended Debye model for **1** at 1 kOe in the temperature range 1.8-6 K.

T / K	$\chi_T / \text{cm}^3 \text{ mol}^{-1}$	$\chi_S / \text{cm}^3 \text{ mol}^{-1}$	$\alpha$	$\tau / \text{s}$	$R^2$
1.8	11.28334	0.29584	0.55069	1.15243	0.9992
2	8.47452	0.32282	0.50101	0.3882	0.9985
2.2	6.39681	0.36337	0.42566	0.13333	0.99749
2.4	5.15287	0.38728	0.34322	0.05663	0.9968
2.6	4.45563	0.39751	0.27547	0.03076	0.99695
2.8	4.0133	0.39113	0.22758	0.01889	0.99743
3	3.68535	0.38194	0.19036	0.01235	0.998

3.5	3.11834	0.3551	0.13334	0.00501	0.99897
4	2.71531	0.32808	0.10228	0.00232	0.99942
4.5	2.43282	0.31037	0.08966	0.00123	0.99965
5	2.36985	0.34282	0.06723	7.17E-04	0.99985
5.5	2.15866	0.33514	0.0622	4.18E-04	0.99988
6	1.98007	0.36744	0.05213	2.50E-04	0.99996

**Table S4.** Best fitted parameters ( $\chi_T$ ,  $\chi_S$ ,  $\tau$  and  $\alpha$ ) with the extended Debye model for **3** at 1 kOe in the temperature range 1.8-3.1 K.

T / K	$\chi_T$ / cm <sup>3</sup> mol <sup>-1</sup>	$\chi_S$ / cm <sup>3</sup> mol <sup>-1</sup>	$\alpha$	$\tau$ / s	R <sup>2</sup>
1.8	0.62201	0.022	0.22699	4.84E-04	0.99986
1.9	0.60163	0.02143	0.23359	4.34E-04	0.99981
2	0.57053	0.02444	0.22366	3.83E-04	0.99983
2.1	0.54422	0.02128	0.21566	3.29E-04	0.9998
2.2	0.51897	0.02638	0.2055	2.93E-04	0.99977
2.3	0.49692	0.05045	0.17347	2.91E-04	0.99982
2.4	0.47786	0.0358	0.17694	2.44E-04	0.99972
2.5	0.45868	0.03727	0.16414	2.17E-04	0.9998
2.6	0.44125	0.03301	0.15421	1.88E-04	0.99975
2.7	0.42678	0.04486	0.14111	1.77E-04	0.99982
2.8	0.40984	0.05935	0.10768	1.70E-04	0.99991
2.9	0.39614	0.05114	0.1078	1.46E-04	0.99987
3	0.38332	0.05057	0.10312	1.30E-04	0.99986
3.1	0.37142	0.04964	0.08941	1.18E-04	0.99993